Analysis of Variance in Neutral Gaze Head Orientation During 3D Head Anthropometry Data Collection

Thomas M. SCHNIEDERS *, Karen BREDENKAMP, Maral DANESHYAN
Magic Leap, Plantation FL, USA

https://doi.org/10.15221/23.22

Abstract

The Frankfurt plane head orientation is widely used in anthropometry research and anthropometric measurement definitions of the whole body and head. However, the authors believe that this head orientation may not be the best for head mounted extended reality (augmented, virtual and mixed reality) devices since it does not relate to natural product wear. When designing head mounted devices (HMDs), it is important to define head orientation, specifically pitch, related to how the device will be worn. In particular, these HMDs are often designed around the eye position with the head and eye in a natural, relaxed orientation - defined in this paper as the “Neutral gaze”. However, the efficacy and repeatability of collecting this posture has not been thoroughly studied. The purpose of this study was to assess the variance of a repeated measures neutral gaze protocol. The primary research questions were: (1) What is the variance in neutral gaze within and between subjects, and (2) what are the largest sources of variance/error? Twelve subjects (four females, eight male) participated in this study. The data collection protocol was repeated five times per subject. Three anatomical landmarks were selected for their resistance to incorrect land marking and measurement - the Left and Right Tragion and the Sellion. Subjects were landmarked, performed a defined series of neck and shoulder stretches, and had their head scanned using a 3dMD® head scanner. Following each scan, subjects stood up, walked up three sets of stairs, performed neck and shoulder stretches, returned to the scanning room, performed neck and shoulder stretches, and an additional head scan was taken. Head scans were digitized in 3dMD Vultus® providing coordinate point locations for the anatomical landmarks under study. This digitization process was conducted three times with proctor A and three times with proctor B to be able to assess intra- and inter-rater reliability. A “Neutral Gaze Vector System” was defined as a user-specified system, where the origin was defined as a point 3 mm in front of the Pupils at the midpoint between the Right and Left Pupil, the x-axis runs through the Right and Left Pupil, the y-axis runs vertically upwards, and the z-axis runs in the anterior direction. MATLAB was used to align all heads to this coordinate system. Variance and range for head pitch were calculated. The authors hypothesized five primary sources of variance: (1) anthropometry land marking, (2) position error of the participant, (3) scanning resolution at the pupil, (4) digitization error, (5) inter- and intra-rater reliability, and (6) MATLAB rotation/translation. Three of these five were investigated in this study. The results indicated the biggest sources of error to be: (1) positioning of the subjects and (2) digitization errors. The result of this work verifies the accuracy and repeatability of the neutral gaze protocol for a product related head orientation. This is especially important when performing such tasks as evaluating form and fit of subjects wearing head mounted devices.

Keywords: 3D face scanning method; method validation; neutral gaze; head orientation; head mounted displays

1. Introduction

The alignment of the head for shape analysis and/or product design remains a challenging topic with few scientists being able to agree on one “true” alignment. This is predominantly due to the head not having a clear long axis such as the whole body, arms, legs, or even feet. In addition, the neck anatomy enables a large range of motion: flexion, extension, and rotation. This challenge of lack of agreement on universal alignment/orientation of the head affects several scientific disciplines from Anthropometry, Anthropology, Dentistry and Orthodontics, Cosmetic Surgery, head wearable product design, and more [3], [4], [10], [11] and [12].

* tschnieders@magicleap.com

In an attempt to agree on one standardized head orientation system, at a World Congress on Anthropology held in Frankfurt am Main, Germany in 1884, a head orientation termed the Frankfurt plane was proposed. In the Frankfurt plane head orientation, a plane passing through the inferior margin of the left orbit (the point called the left orbitale) and the upper margin of each ear canal or external auditory meatus, a point called the Porion, was most nearly parallel to the surface of the Earth at the position the head is normally carried in the living subject. This definition is widely adopted in the field of Anthropometry as the head oriented such that the Orbitale and Tragion anatomical landmarks are on the same horizontal plane [1].

Several different head orientations have been applied during data collection of 1D or 3D head Anthropometry. During the SizeChina-Hunan 3D head anthropometry data collection, the head orientation of participants being scanned was defined by participants being instructed to look at a fixed point marked in front of them [2], [3]. A similar head orientation protocol was used when capturing 3D head scans for Australian bicycle helmet design [4]. During the 3D head anthropometry data collection for the Korean population, the heads were oriented in the Frankfurt plane in accordance with postures described in ISO 20685-1 [5], [6]. The Frankfurt plane head orientation was furthermore also used during the Japanese [7], South African military [8] and US military [9] 3D head anthropometry data collection projects.

ISO 20685-1 [5] 3D scanning methodologies for international compatible anthropometric databases Part 1 recommends, among other topics, standardized postures for 3D body scanning when building a 3D anthropometric database. ISO 20685-1 [5] suggests 4 postures for body scanning, with the head alignment in all of them recommended to be in the Frankfurt plane. The Frankfurt plane was defined as the head pitched such that the right Infraorbitale landmark below the eye is on the same horizontal plane as the right Tragion landmark, and that the head is yawed such that the right and left Tragion landmarks are on a horizontal plane.

In the attempt to understand and define shape variances of the head for application to product design and/or evaluation, several researchers have investigated and suggested different head orientations. In classifying the human skull morphology, [10] takes advantage of 3D imaging and digitization techniques and recommends using 3D Procrustes superimposition as a method of determining head orientation and alignment. Procrustes superimposition is an iterative least-square adjustment of all the figures after size normalization. It includes three phases: scaling, translation, and rotation. The skulls are scaled to have the same size, they are translated to have their geometrical centers fit exactly with one another, and finally, rotated in order to minimize the gaps between anatomical points.

Badawi-Fayad and Cabanis [10] used the x, y, z coordinates of 33 anatomical landmark points as input to the Procrustes alignment. During the SizeChina-Hunan head scanning project, after data collection, the head scans were digitally processed during which each head scan was rotated and translated into the Frankfurt plane. With the x-axis running through the left and right Tragion landmarks, origin located midway between the left and right Tragion, and positive direction towards the right Tragion. The XOY plane passed through the left and right Tragion, and left Infraorbitale landmarks. Positive y-direction anteriorly and positive z-direction upwards [2], [3]. Park et al. [11] aligned 180 3D head scans in order to create a parametric adult head model with representation of scalp shape variability. These head models were aligned in the Frankfurt plane for statistical analysis. The coordinate system was defined with origin midway between the left and right Tragion, the y-axis running through right and left Tragion landmarks. The XOY plane passed through the left and right Tragion and the left Infraorbitale landmarks. The z-axis is a cross product of x- and y-axes, running vertical. Gupta et al. [12] aligned 3D face scans as part of building a face recognition database. After data capture, the face scans were aligned with the forehead tilted back by 10 degrees to the vertical axis. This was achieved by iteratively aligning facial models in arbitrary poses to a template face in a canonical frontal pose using the Iterative Closest Point (ICP) algorithm [12], [13].

Niezgoda and Zhuan [14] analyzed the shape variance of approximately 400 head scans of the United States civilian population for the purpose of creating headforms for ISO Eye and Face Protection Standards. In order to analyze variance of the head and face shape and sizes, they aligned all heads in the Frankfurt plane [14]. Digital 3D headforms representative of Chinese workers were aligned in the Frankfurt plane (horizontal plane) and vertical plane passing through 3 midpoints, between right and left Tragion, right and left Zygion, and right and left Ectocanthus [15].

In the absence of one consistent head orientation and coordinate system, Lee et al. [16] investigated multivariate statistical shape variances for several different coordinate system origins. The head scans were oriented with the x-axis passing through the left and right Tragion landmark points, and the y-axis passing through the Sellion and Supramentale landmarks. The different coordinate system origins included 1) Sellion landmark, 2) Pronasale landmark, and 3) midway between right and left Tragion landmarks. For the origin located at the midpoint between right and left ear, the largest percentage of variance was described by the 3 principal components (PC's) (89.7%), compared to the other two origin points (76.3% and 76.9%, respectively). Different results are expected if the head scans were orientated in the Frankfurt plane. In a study during which 3D face scan data was used for the analysis of facial size and shape, Lee et al. [17] aligned all the faces with the origin at the Sellion landmark, and the y-axis passing through the Sellion and Supramentale landmark, and the x-axis parallel to a line passing through the left and right Tragion landmarks.

Robinette [18] summarizes several alignment frameworks investigated for head alignment for helmet applications. These included: 1) the Principal Axis System (PrinAx), 2) an approximate coronal plane alignment (Eye), and 3) a top-of-head alignment. For all three alignment frameworks, the head rotational orientation (pitch, roll, and yaw) was the same, with the main point of difference being the origin of the Cartesian system. For the PrinAx, the surface area of the triangles of the polygon file were used as mass (constant density assumed), and the center of mass (calculated for all the triangles) was used as the origin of the coordinate axis. For Eye, the origin was midway between the right and left eye, and for top-of-head alignment, the origin was at the most superior point on the head.

Although the Frankfurt plane is most widely used by researchers when analyzing or attempting to represent shape variances of a population group's heads and faces, a universal consensus has still not been reached. It is the author's opinion that a universal head orientation and alignment that is in line with how the product will be worn on the head or face. This would mean that for head models used for design, different head models will be required for different head and face products. An "universal" head model in one set head alignment will most likely provide a false sense of representation of head and face variance, since inevitably head orientation artifacts, such as forward-backward rotation (pitch), which might not be applicable to how the product is worn, would be reflected in some of the shape variance components. A careful understanding of how the product is expected to be worn, must therefore be formulated before the head orientation is selected. This understanding could be formulated through an informal, small scale fit test of similar products. With the use of software tools, 3D head data can be re-oriented to the desired head orientation with relative ease.

For the design of the Magic Leap headset, a head orientation in a natural head position was selected as best suited to the headset design. This head orientation is termed "Neutral Gaze" head orientation. When obtaining a head scan with the head in this orientation, a consistent process was used to position each participant in this intended head orientation position. This process included specific neck and shoulder stretches, requesting the participant to sit upright with shoulders back and down, and look at himself/herself in a mirror placed on a vertical plane 2m in front of the participant.

The purpose of this study was to investigate the consistency of this head orientation and the repeatability with which participants are able to position themselves in this "Neutral Gaze" head orientation position.

2. Method

Participants were required to sign an informed consent and were not compensated monetarily or otherwise for participating. Left and right Tragion anatomical landmark locations were visually identified by trained proctors using an eyeliner pencil. Participants were seated on a chair within the scanning volume of a 3DMD scanner. To ensure subjects were in a neutral position, they were instructed to flex and extend their neck ("Look down to your chest, look up to the ceiling"), rotate their neck ("Look left to the wall next to you, look right at the wall on the opposite side"), bend their neck sideways ("Bend your neck to the side, as if to touch your ear to your shoulder, first to the left shoulder then to the right shoulder") , and finally asked to sit with their back straight and roll their shoulders backwards and down. They were then instructed to stare straight ahead while looking at themselves in a mirror mounted vertically in front of them. A 3D image was captured using a 3dMDhead™ system.

Following this, the subjects were led outside of the scanning room to a movable staircase that had 3 steps and a railing. They were instructed to hold onto the railing while ascending the stairs. At the top of the stairs they were again instructed to flex and extend, rotate left and right, and bend to the left and right their neck, and roll their shoulders back and down. They were then instructed to hold the railing as they descended the stairs where they returned to the scanning room. They repeated this method for a total of five collections. The same set of markings indicating the landmarks was used in all five collections.

Land marking

The purpose of this study was to assess the precision and repeatability of a neutral gaze head orientation methodology. To measure relative change in neutral gaze, three anatomical landmarks were chosen for their ease of marking and their resistance to incorrect marking (i.e. bony protrusion with resilience against fatty deposits or skin stretching). The left Tragion, the right Tragion, and the Sellion were chosen (see Figure 1).

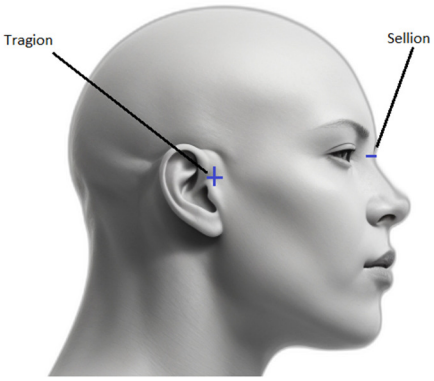

Figure 1: Tragion and Sellion

Head Motions of Interest

In order to calculate variability in the neutral gaze angle, it is important to correctly identify the head motions of interest. There are three rotational head motions: (1) yaw, (2) roll, and (3) pitch (see Figure 2). Yaw is defined as rotation about the y-axis and in head motion is seen as shaking the head no. Roll is defined as the rotation about the z-axis and is seen as tilting the head from side to side. Pitch is defined as rotation about the x-axis and is seen as nodding the head up and down. In addition, there are combinatorial head motions (e.g. yaw + pitch) but those are excluded in this study. For this investigation, the analysis was confined to the effect of the neutral gaze protocol on the pitch head motion only. Each head scan is post-processed using MATLAB code [19]. For each individual's head scan, the origin of the scan varies depending on each day's scanner calibration, and is originated relative to the scanner volume, and not the head. The MATLAB code is used to translate and rotate all data such that the right and left Corneal Apex points are coplanar and horizontal relative to one another on the XOY plane, and the origin is positioned midway between the left and right Corneal Apex points. The Corneal Apex points are estimated as 3 mm anterior to the pupil positions. This process minimizes the effect of roll and yaw to zero for the purposes of this analysis. Proof of this process is explored later in this paper.

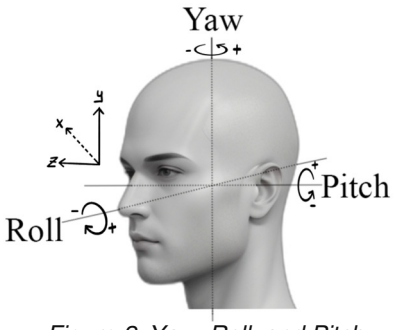

Figure 2: Yaw, Roll, and Pitch

Calculation of Pitch

Of interest in this analysis was the variation in neutral gaze pitch angle. One method to analyze this was to look at the variability in pitch angle between the Tragion and Sellion landmarks. To complete this calculation, an artificial point was created containing the y-coordinate position of the Tragion of interest (either left or right) and the x- and z-coordinate position of the Sellion (see Figure 3).

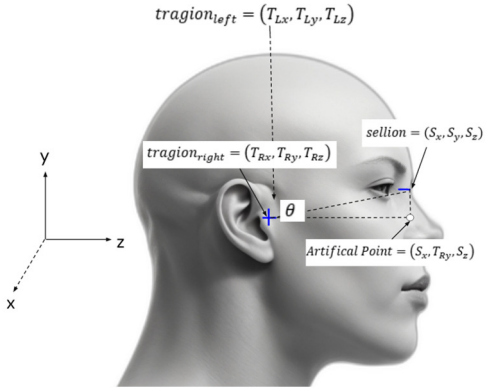

Figure 3: Pitch calculation

Calculations for pitch between left Tragion and Sellion, as well as right Tragion and Sellion must be done. This is due to variability within human morphology as well as the possibility of variance in land marking and digitization. As such, the calculations used for left and right pitch can be found below.

$$Pitch_{left} = \tan^{-1}\left(\frac{S_y - T_{Ly}}{S_z - T_{Lz}}\right) \quad (1)$$

$$Pitch_{right} = tan^{-1}\left(\frac{S_y - T_{Ry}}{S_z - T_{Rz}}\right) \quad (2)$$

3. Results and Discussion

Participants were individuals above the age of 18 who could legally give consent and worked at the same company where the collection was taking place. Twelve participants completed the study with five collections per participant. Twelve participants completed the study with five repeated scans and two Proctors digitizing each scan three times. For each participant, Proctor 1 always landmarked the left and right Tragion and Proctor 2 always carried out the head scan methodology. This was done to ensure inter-Proctor variability was eliminated for the anatomical land marking and the delivery of methodology instruction. The data for one participant had missing information and was removed from the analysis.

Data distribution

Each of the 12 subjects had five head scans with six digitizations (three digitized by Proctor 1 and three digitized by Proctor 2). One of the subjects only had four head scans due to data corruption. Therefore, each subject had 30 data points. The normalized pitch angles for all the data points (6 digitizations for each of the 5 scans) for each participant is plotted in Figure 4. This relative difference is used to create a ‘zero point’ such that the spread of variance in pitch can be viewed on the same axes. When referring specifically to statistical analyses related to pitch moving forward, all values will be based off of the normalized median zero point. All analyses and discussions will be relative to that value.

The standard deviation of pitch values for each of the data points were calculated per participant. The Calculations for the mean, minimum, and maximum variance for both the left and right pitch values were completed. The mean, minimum, and maximum range of the variance was also calculated.

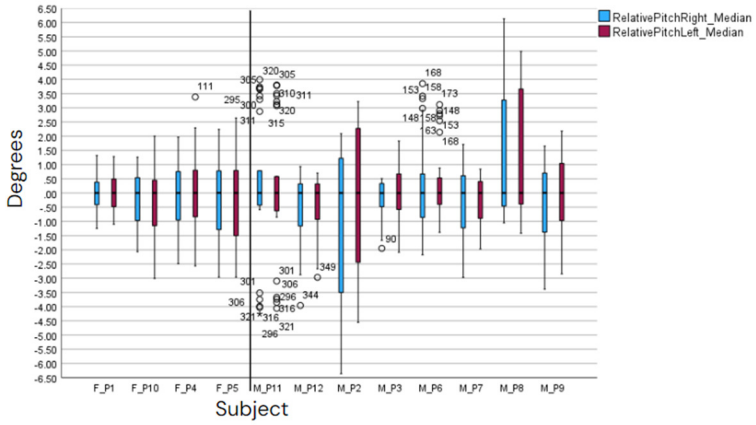

Figure 4: Normalized Relative Pitch

The variance and standard deviation for the six digitizations of each scan was calculated for both the left and right pitch angle. This is summarized in Table 1. The table includes the minimum, maximum, and mean for standard deviation and variance calculated from the normalized pitch angles. In addition, the table includes the minimum, maximum, and mean of the range of those pitch angles. From a practical standpoint, we will use the values of range to describe the variance in pitch. The standard deviation across the 30 observations for each of the 12 participants. The minimum, mean, and maximum standard deviation is across the 12 participants.

Table 1: Standard deviation between 12 participants

Pitch left		**Pitch Right**	
Mean σ	1.45	Mean σ	1.50
Min σ	0.39	Min σ	0.69
Max σ	2.40	Max σ	2.67

The authors posit that there are six main sources of error that could contribute to the variance in the neutral gaze head orientation: 1) anthropometry land marking, 2) positioning error of the participant, 3) scanning resolution at the pupil, 4) digitization error, 5) inter-rater and intra-rater (digitization) reliability, and 6) translation in MATLAB.

Anthropometry land marking error

This could most likely be the largest source of inter-participant variance, but was not included in this study. This source of variance was intentionally omitted because the main objective of the study was to understand the error from the position of the subject. Between all data collection runs per participant, each participant was landmarked once, and the same set of markings were used in the repeated scans and repeated digitization per each proctor. Proctor 1 always landmarked the subject while Proctor 2 always carried out the head scan protocol.

Positioning error

This is most likely the second largest contributor to both inter- and intra-subject variance. Understanding the magnitude of this source of variance is one of the primary objectives of this study. Variance is also due to the repeatability of the subject to position themselves in the neutral gaze head orientation.

To simulate the natural variance created from repositioning subjects into neutral gaze inside of the scanner volume, subjects were given a body break, which included: standing up, walking out of the scanner room, walking up stairs, stretching neck and shoulders, walking down stairs, and returning to the scanner room.

To evaluate how much positioning error contributes to the overall variance, the left and right pitch angles were grouped by scan - therefore, each participant has five scans, and each scan has six digitizations yielding 30 data points. For each scan, the average was calculated for the six digitizations producing five averages for the left pitch angle and five averages for the right pitch angle. The median value for the left and right pitch angles was calculated. The left and right average pitch was then normalized. This allows for the calculation of an average of the pitch angles to be calculated. In a practical sense, this means positioning error consists of the mean plus/minus three standard deviations. Again, to look at the worst case scenario, we will take the largest values. Variance due to participant positioning error is 0.36 ± 5.83˚. A summary of the data can be found in the table below.

Table 2: Position error contribution

	AverageLeft	AverageRight	MedianLeft	MedianRight	RelativeLeft	RelativeRight		AverageLeft	AverageRight	MedianLeft	MedianRight	RelativeLeft	RelativeRight
P1_Scan1	13.29	10.75			-0.79	-1.18	P7_Scan1	18.81	19.09			0.00	0.00
P1_Scan2	14.08	11.93			0.00	0.00	P7_Scan2	19.29	20.02			0.49	0.93
P1_Scan3	14.91	12.63	14.08	11.93	0.83	0.70	P7_Scan3	18.07	18.98	18.81	19.09	-0.74	-0.10
P1_Scan4	13.84	11.35			-0.25	-0.58	P7_Scan4	19.34	19.73			0.53	0.65
P1_Scan5	14.47	11.94			0.39	0.01	P7_Scan5	17.14	18.08			-1.67	-1.01
P2_Scan1	11.43	10.36			1.07	-4.81	P8_Scan1	20.38	20.49			-0.17	0.00
P2_Scan2	13.59	12.75			3.23	-2.42	P8_Scan2	20.55	20.35			0.00	-0.14
P2_Scan3	16.64	16.61	14.99	15.17	6.28	1.44	P8_Scan3	20.12	20.44	20.55	20.49	-0.43	-0.05
P2_Scan4	17.55	16.86			7.19	1.69	P8_Scan4	24.75	22.75			4.20	2.26
P2_Scan5	14.99	15.17			4.63	0.00	P8_Scan5	24.44	23.94			3.89	3.45
P3_Scan1	23.99	25.36			0.02	0.00	P9_Scan1	21.75	22.33			-2.55	-3.05
P3_Scan2	23.03	25.00			-0.95	-0.36	P9_Scan2	25.36	25.87			1.06	0.48
P3_Scan3	24.59	25.57	23.97	25.36	0.62	0.20	P9_Scan3	23.61	24.32	24.30	25.38	-0.69	-1.06
P3_Scan4	23.97	25.59			0.00	0.23	P9_Scan4	25.37	25.50			1.07	0.12
P3_Scan5	21.94	23.86			-2.04	-1.50	P9_Scan5	24.30	25.38			0.00	0.00
P4_Scan1	22.58	22.74			0.98	2.21	P10_Scan1	18.37	19.17			0.07	0.96
P4_Scan2	20.68	20.52			-0.92	0.00	P10_Scan2	16.40	16.95			-1.90	-1.26
P4_Scan3	21.59	20.48	21.59	20.52	0.00	-0.04	P10_Scan3	17.14	17.69	18.30	18.21	-1.17	-0.51
P4_Scan4	21.60	21.04			0.01	0.51	P10_Scan4	19.43	18.48			1.13	0.28
P4_Scan5	19.41	19.05			-2.18	-1.47	P10_Scan5	18.30	18.21			0.00	0.00
P5_Scan1	12.49	12.23			0.43	0.10	P11_Scan1	16.27	16.60			3.51	3.55
P5_Scan2	11.65	12.03	12.07	12.13	-0.41	-0.10	P11_Scan2	10.35	10.19			-2.41	-2.86
P5_Scan3	12.48	12.40			0.41	0.27	P11_Scan3	13.02	13.23	12.76	13.05	0.26	0.18
P5_Scan4	9.94	9.81			-2.13	-2.32	P11_Scan4	12.76	13.05			0.00	0.00
P6_Scan1	26.61	28.99			0.00	0.00	P11_Scan5	12.40	12.76			-0.36	-0.29
P6_Scan2	25.93	28.70			-0.68	-0.29	P12_Scan1	14.65	14.65			0.00	0.00
P6_Scan3	26.94	29.62	26.61	28.99	0.33	0.63	P12_Scan2	14.46	13.55			-0.19	-1.10
P6_Scan4	29.34	31.07			2.73	2.08	P12_Scan3	15.07	14.94	14.65	14.65	0.42	0.29
P6_Scan5	26.28	27.27			-0.33	-1.72	P12_Scan4	15.20	14.77			0.56	0.12
							P12_Scan5	12.53	11.86			-2.11	-2.79

Average of Relative Left	0.36		
Average of Relative Right	-0.13		
SD of Raw Left	1.94	3xSD of Raw Left	5.83
SD of Raw Right	1.44	3xSD of Raw Right	4.33

Scanning resolution at the pupil error

There is inherent uncertainty and variance found in the digitization process. One major component of this variance comes from the scanner resolution. This resolution directly impacts the number of points the scanner creates especially for certain areas. Each time a scan is taken, the number of scan points and the location of the scan points generated may vary. This is especially important when looking at the point array for landmarks which may differ even within the same subject in the same trial. One factor that severely affects the scanning resolution and point accuracy is the surface color and finish since the scanner technology relies on how well the light pattern projected on the object is reflected back to the camera's. Very dark to black surface colors scan very poorly since the light projected on the object is absorbed. Shiny surface finishes furthermore scans very poor since the light projected on the object is reflected, resulting in stray scan points.

This makes scanning the pupil accurately, especially for a person with dark irises, very difficult. This poor scan point distribution then also makes identifying the exact center of the pupil problematic (see Figure 5). Furthermore, the point array that represents the subjects' eyes has a lower vertex count.

Scanner technology does not collect dark or reflective objects well and digitization in those regions is seen as unreliable. This is inherently a large problem when dark colored eyes are predominant in most countries (45% in the US, and >50% worldwide) [20]–[22]. This is especially prominent for certain ethnic (i.e. Asian and Black). This is further investigated in the digitization error section.

Figure 5: Digitization of dark brown eye

Digitization error

Proctor digitization variance is another major component of variance in the digitization process. This is impacted by multiple factors such as how "zoomed in" the proctor is during the digitization process, the angle and rotation of the head scan, the resolution and lighting of the monitor the proctor is using, ambient lighting, and fatigue. Additional factors include how accurate the proctor is during the selection of landmarks as well as the inherent tradeoff between speed, precision, and accuracy.

Additional variance in this process includes general software considerations. In the case of this study we will discuss scan alignment in 3dMD Vultus™ [23]. The headscan will not always import correctly from the 3dMDhead™ scanner or be correctly aligned to the center. Figure 6 demonstrates a headscan that is in the "right side view" according to 3dMD Vultus™ [23], however this is clearly the "front view" of the subject. Outside of the wrong view alignment by the digitization software, the subject is also inaccurately placed into a tilted view. This leads to a large discrepancy in raw coordinate positions for matching anatomical points (i.e. left and right Tragion). The digitizer must also manually rotate the head scan and with the version used, there is no way to lock rotation along one axis. However, this error should be accounted for with the neutral gaze MATLAB code. This issue can still significantly impact the digitizers' ability to accurately digitize anatomical points. This is especially true for landmarks (i.e. the Sellion) that are not physically marked but are found in the digitization process.

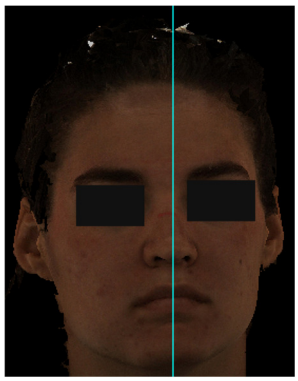

Figure 6: Headscan tilt

It was previously hypothesized that a large contribution to the variance was the error caused by the scanning resolution at the eye. This variance was evaluated by Proctor 2 by using the same head scan, selecting the left and right Tragion, Sellion, and left and right Pupils ten times. This was followed by calculating the uncertainty in measurement at the Sellion, Tragion, and Pupil. The headscan chosen for evaluation had dark brown / black eyes to create a worst case scenario for digitization error. It was found that the uncertainty in measurement for the angle created between the Tragion, Sellion, and horizontal was 0.79 degrees (see Table 3).

Table 3: Uncertainty in measurement

Case	SellionX	SellionY	SellionZ	TragionRX	TragionRY	TraionRZ	PupilRX	PupilRY	PupilRZ	PitchR
1	9.48	8.67	122.28	-84.54	-14.59	44.92	-28.15	4.95	115.17	16.73
2	9.81	8.99	122.1	-84.44	-13.94	43.24	-28.29	4.98	115.17	16.21
3	10.45	8.67	122.15	-85.06	-14.59	43.95	-28.29	4.66	115.21	16.56
4	10.13	8.99	122.06	-86.43	-14.91	43.69	-28.01	5.12	115.13	16.96
5	10.13	9.64	121.82	-84.89	-15.23	44.28	-28.29	4.59	115.21	17.78
6	9.81	8.99	122.1	-86.11	-14.91	42.34	-28.15	4.43	115.22	16.68
7	10.45	9.31	121.9	-84.7	-14.27	44.6	-27.67	4.43	115.2	16.96
8	9.81	9.31	121.97	-85.65	-14.91	42.98	-27.53	4.59	115.17	17.05
9	9.81	9.31	121.97	-85.67	-15.56	42.98	-27.91	4.04	115.23	17.48
10	10.13	9.31	121.94	-84.89	-15.23	44.28	-28.58	4.38	115.18	17.54
Mean	10.001	9.119	122.029	-85.238	-14.814	43.726	-28.087	4.617	115.189	17.00
Uncertainty	0.485	0.485	0.23	0.995	0.81	1.29	0.525	0.54	0.05	0.79
Final	10.001+/-0.485	9.1+/-0.5	122.03+/-0.23	-85.2+/-1	-14.8+/-0.8	43.7+/-1.3	-28.09+/-0.53	4.6+/-0.5	115.2+/-0.1	17+/-0.79

It is shown that the original hypothesis of the largest contribution to the variance was the error caused by the scanning resolution at the eye is in fact incorrect. However, it is believed this low uncertainty in the pupil is not the full picture. As discussed in the previous section, there is a lower vertex count in the pupil. It is believed that the digitization process is forcing a Pupil landmark to be selected among a smaller set of vertex points leading to an artificially higher precision which could lead to a lower accuracy of the true measure. However, this investigation is outside of the scope of this paper.

Inter-rater and intra-rater reliability

For intra-rater reliability, that is, variance within one proctor, the variance was calculated and compared between the Proctor's individual runs. For inter-rater reliability, the variance between proctors, the variance between Proctor 1 and Proctor 2 was compared between runs. Variance can be expected to be more than 10% between proctors and random error due primarily to ambiguity in the landmark (i.e. soft tissue, exact pupil center, etc.) [24]. This inter-rater and intra-rater reliability analysis was completed for pitch, left Tragion (x, y, z), right Tragion (x, y, z), and Sellion (x, y, z).

Neutral gaze translation in MATLAB

For the process used in this study, this is believed to be a negligible source of error. The MATLAB code translates and rotates the coordinates of each subject such that the pupils are coplanar and horizontal relative to one another. This is done under the assumption that humans are different and varied! It is rare for human facial morphology to be completely symmetrical and this should be taken into consideration during the land marking and digitization processes. This rotation and translation helps to eliminate natural yaw and roll rotations during head scanning.

To validate that this was a negligible source of variance, the MATLAB code was applied five times on the same set of data. There was no difference in landmark location between the five sets of data. Therefore, the authors posit that no variance is introduced from the MATLAB translation and rotation.

4. Conclusions and Recommendations

While research has been done on head alignment for shape analysis and/or product design, no consensus is reached among researchers on the one "true" head alignment. Head alignment impacts multiple disciplines and requires additional research on specific head alignments as well as the repeatability of positioning participants in each specific alignment. The repeatability of positioning participants in the "Neutral gaze" head alignment was determined in this study. One method that was

investigated in this paper is the neutral gaze collection on 12 adults with 5 observations each was conducted and the variance in neutral gaze was investigated as well as errors that contribute to that variance. Average variance in the neutral gaze head alignment is ~3 degrees squared with a maximum variance for this data set calculated as ~11 degrees. In practical application, this equates to an average standard deviation of ±1.6 degrees with a potential for as much as 3.3 degrees and this should be accounted for when designing head mounted equipment.

The authors identified six factors that are expected to influence variance: 1) anthropometry land marking, 2) position error of the participant, 3) scanning resolution at the pupil, 4) digitization errors, 5) inter- and intra-rater reliability, and 6) MATLAB rotation/translation.

It was assumed that the neutral gaze alignment process is not dependent on gender and/or ethnicity, however this should be validated with a larger sample size that targets those demographics.

Additional analysis should be conducted on inter-rater and intra-rater reliability as it specifically relates to head anthropometry used in multiple head alignment processes. It has been shown that this is the largest source of error contributing to the variance in the neutral gaze alignment. With additional training, it is possible to reduce this contributing factor. The Proctors were trained by an anthropometrist and have 3 years or less of experience conducting anthropometry related collections as it pertains to head measurements.

References

[1] International Society for the Advancement of Kinanthropometry, *Advanced Kinanthropometry (ISAK)*. 2001. [Online]. Available: http://www.isakonline.com/

[2] H. Wang, W. Yang, Y. Yu, W. Chen, and R. Ball, “3D Digital Anthropometric Study on Chinese Head and Face,” presented at the Proc. of 3DBODY.TECH 2018 - 9th Int. Conference and Exhibition on 3D Body Scanning and Processing Technologies, Lugano, Switzerland, 16-17 Oct. 2018, Oct. 2018. doi: 10.15221/18.287.

[3] Y. Luximon, R. Ball, and E. Chow, “A design and evaluation tool using 3D head templates,” *Comput.-Aided Des. Appl.*, vol. 13, pp. 1–9, Sep. 2015, doi: 10.1080/16864360.2015.1084188.

[4] T. Perret-Ellena, S. L. Skals, A. Subic, H. Mustafa, and T. Y. Pang, “3D Anthropometric Investigation of Head and Face Characteristics of Australian Cyclists,” *Procedia Eng.*, vol. 112, pp. 98–103, Jan. 2015, doi: 10.1016/j.proeng.2015.07.182.

[5] ISO 20685-1, *ISO 20685-1:2018. 3-D scanning methodologies for internationally compatible anthropometric databases -- Part 1: Evaluation protocol for body dimensions extracted from 3-D body scans*. 2018. Accessed: Nov. 29, 2018. [Online]. Available: http://www.iso.org/cms/render/live/en/sites/isoorg/contents/data/standard/06/32/63260.html

[6] “sizeKorea.” https://sizekorea.kr/ (accessed Sep. 15, 2023).

[7] M. Kouchi and M. Mochimaru, “Analysis of 3D face forms for proper sizing and CAD of spectacle frames,” *Ergonomics*, vol. 47, no. 14, pp. 1499–1516, 2004.

[8] RSA-MIL-STD 127 Vol 1, “Ergonomics design: Anthropometry and Environment.” ARMSCOR, Pretoria, South Africa, 2005.

[9] J. Hotzman *et al.*, “Measurer’s Handbook: US Army and Marine Corps Anthropometric Surveys, 2010-2011,” Aug. 2011. Accessed: Sep. 15, 2023. [Online]. Available: https://www.semanticscholar.org/paper/Measurer%27s-Handbook%3A-US-Army-and-Marine-Corps-Hotzman-Gordon/142e48d32b83739ca0c9aa88e0b7aca517dc50b4

[10] J. Badawi-Fayad and E.-A. Cabanis, “Three-dimensional Procrustes analysis of modern human craniofacial form,” *Anat. Rec. Hoboken NJ 2007*, vol. 290, no. 3, pp. 268–276, Mar. 2007, doi: 10.1002/ar.20442.

[11] B.-K. D. Park, B. D. Corner, J. A. Hudson, J. Whitestone, C. R. Mullenger, and M. P. Reed, “A three-dimensional parametric adult head model with representation of scalp shape variability under hair,” *Appl. Ergon.*, vol. 90, p. 103239, Jan. 2021, doi: 10.1016/j.apergo.2020.103239.

[12] S. Gupta, M. Markey, and A. Bovik, “Anthropometric 3D Face Recognition,” *Int. J. Comput. Vis.*, vol. 90, pp. 331–349, Dec. 2010, doi: 10.1007/s11263-010-0360-8.
[13] S. Gupta, K. Castleman, M. Markey, and A. Bovik, *Texas 3D Face Recognition Database*. 2010, p. 100. doi: 10.1109/SSIAI.2010.5483908.
[14] G. Niezgoda and Z. Zhuang, “Development of Headforms for ISO Eye and Face Protection Standards,” *Procedia Manuf.*, vol. 3, pp. 5761–5768, Dec. 2015, doi: 10.1016/j.promfg.2015.07.822.
[15] Y. Yu *et al.*, “Digital 3-D Headforms Representative of Chinese Workers,” *Ann. Occup. Hyg.*, vol. 56, pp. 113–22, Sep. 2011, doi: 10.1093/annhyg/mer074.
[16] W. Lee *et al.*, “Application of massive 3D head and facial scan datasets in ergonomic head-product design,” *Int. J. Digit. Hum.*, vol. 1, p. 344, Dec. 2016, doi: 10.1504/IJDH.2016.10005368.
[17] W. Lee, L. Goto, J. Molenbroek, and R. Goossens, *Analysis Methods of the Variation of Facial Size and Shape Based on 3d Face Scan Images*, vol. 61. 2017, p. 1413. doi: 10.1177/1541931213601836.
[18] K. M. Robinette, “Maximizing anthropometric accommodation and protection,” Air Force Research Laboratory, Biomechanics Branch, Wright-Patterson Air Force Base, Ohio, Technical Report, 2007. [Online]. Available: https://apps.dtic.mil/sti/pdfs/ADA478783.pdf
[19] “MATLAB.” The MathWorks, Inc., 2019.
[20] M.-A. Katsara and M. Nothnagel, “True colors: A literature review on the spatial distribution of eye and hair pigmentation,” *Forensic Sci. Int. Genet.*, vol. 39, pp. 109–118, Mar. 2019, doi: 10.1016/j.fsigen.2019.01.001.
[21] G. Prota, D.-N. Hu, M. R. Vincensi, S. A. McCORMICK, and A. Napolitano, “Characterization of Melanins in Human Irides and Cultured Uveal Melanocytes From Eyes of Different Colors,” *Exp. Eye Res.*, vol. 67, no. 3, pp. 293–299, Sep. 1998, doi: 10.1006/exer.1998.0518.
[22] A. R. Wielgus and T. Sarna, “Melanin in human irises of different color and age of donors,” *Pigment Cell Res.*, vol. 18, no. 6, pp. 454–464, 2005, doi: 10.1111/j.1600-0749.2005.00268.x.
[23] “3dMD Vultus.” 3dMD, 2017.
[24] M. Kouchi and M. Mochimaru, “Errors in landmarking and the evaluation of the accuracy of traditional and 3D anthropometry,” *Appl. Ergon.*, vol. 42, no. 3, Art. no. 3, Mar. 2011, doi: 10.1016/j.apergo.2010.09.011.

Author Information

Dr. Thomas M. Schnieders, Ph.D., A. Eng, AEP is a Senior Human Factors Engineer at Magic Leap, USA, Co-Founder of The ATHENA Lab, and Co-Founder of The Society of Augmented Engineers and Scientists, Inc. He received his PhD in Industrial Engineering and Statistics from Iowa State University in 2019; his MS in Industrial Engineering and Human-Computer Interaction from Iowa State University in 2016; and his BS in Mechanical Engineering in 2014. His current research focuses on human factors and ergonomics test protocols centered on understanding areas of fit, comfort, and performance for head mounted augmented reality headsets. He has backgrounds in human performance engineering as it relates to exoskeleton design, manufacturing, and testing, tool design, classic ergonomic evaluation, tele-robotic technology, biomechanical engineering, drone technology, and virtual reality.

Karen Bredenkamp is a Principle Human Factors Engineer at Magic Leap, USA and co-chair of the Anthropometry TC for the International Ergonomics Association (IEA). In her current role, she heads up the Human Factors group within Magic Leap, oversees the 3D head anthropometry database and conducts research and user testing as part of the product design process. Before that, Karen was a Chief Engineer at ERGOTECH, a Division of Armscor, South Africa, with a main focus on conducting Human Factors and Ergonomics research for the South African National Defence Force (SANDF), South African military industry partners, government organizations in transportation and safety industries, as well as mining and commercial clients. Here she had a leading role in the establishment of the first and largest 3D whole-body, head and foot anthropometric databases in South Africa, and Africa, and conducted anthropometry and biomechanics research as part of product design and evaluation. Karen received her M.Sc. in Biomedical Engineering from the University of Cape Town and B. Ing Mechanical Engineering degree from the University of Stellenbosch in South Africa.